Chin. J. Astron. Astrophys. Vol. 6 (2006), No. 6, 723–728
(*http://www.chjaa.org*)

Chinese Journal of
Astronomy and
Astrophysics

The Magnetic Field Effect on Planetary Nebulae

A. R. Khesali[1,2] and K. Kokabi[1]

[1] Department of Physics, University of Mazandaran, Babolsar, Iran; *khesali@umz.ac.ir*
[2] Research Institute for Astronomy and Astrophysics of Maragha, Maragha, Iran

Received 2005 December 28; accepted 2006 October 11

Abstract In our previous work on the 3-dimensional dynamical structure of planetary nebulae the effect of magnetic field was not considered. Recently Jordan et al. have directly detected magnetic fields in the central stars of some planetary nebulae. This discovery supports the hypothesis that the non-spherical shape of most planetary nebulae is caused by magnetic fields in AGB stars. In this study we focus on the role of initially weak toroidal magnetic fields embedded in a stellar wind in altering the shape of the PN. We found that magnetic pressure is probably influential on the observed shape of most PNe.

Key words: ISM: Planetary nebulae – magnetic field: PNe – magnetic field

1 INTRODUCTION

Only a small fraction of the observed planetary nebula (PN) population has spherical structure. Most PNe possess asymmetrical structures in a rich variety of morphologies that are frequently observed (Balick 1987). It is widely accepted that the PNe are powered by line-driven winds emerging from their central stars and formed from a two-wind dynamic interaction (Kwok et al. 1978). Evidence for this scenario comes from the large number of P-Cygni line profiles detected in their central objects (Perinotto 1983). One of the major open questions is "which mechanism is responsible for their asymmetrical structure?" Many factors can break the spherical symmetry. Either external torques of a closed or merging binary companion or the emergence of magnetic fields embedded in dense out flowing stellar winds can be responsible for these structures.

As proposed, the bipolar structure is related to a toroidal magnetic field in the wind of central star (Pascoil 1997). This idea has been reinforced by the discovery of magnetic fields in AGB stars (Etoka & Diamond 2004) and more recently in actual stars of PNe (Jordan et al. 2005).

In this paper, we took a physical mechanism based on interacting winds and considered magnetic effects in the shocked stellar wind. We assumed a gas pressure and a magnetic pressure transported out from the interior shell to its surface and a suitable density for the ambient gas. The result is an elongated nebula, as shown by variation of the expansion velocity at the different angles. In Section 2, we explain the role of the effect of magnetic fields in shaping the PNe. In Section 3, we describe the theoretical model and use of the thin shell approximation in the dynamical study of PNe. In Section 4 by considering a magnetic field, we apply our method to PNe. We summarize our results in Section 5.

2 THE ROLE OF MAGNETIC FIELDS IN SHAPING PNE

Four categories exist for explaining the role of magnetic field in shaping PNe.

(1) Magnetic pressure is dynamically important on the AGB stellar surface (Pascoli 1997; Matt et al. 2000; Blackman et al. 2001).
(2) The magnetic field plays a dynamical role at a large distance from the star, but it is weak close to the AGB stellar surface (Chevalier & Luo 1994; Garcia-Segura et al. 1999).

(3) Magnetic fields never become dynamically important on large scales (Soker 2004).
(4) Magnetic fields play a dominant role in the launching of jet from accretion disks, either around stellar companions or the central star, the action of the jets shapes the PNe.

Each of the processes has a low and high point. We consider a stellar wind with a constant mass-loss rate $\dot{M}$ and a constant terminal wind velocity. The basic assumption is that the magnetic field is carried by the flow.

We take the magnetic field components in the equatorial plane at distance r from the stellar center (Chevalier & Luo 1994),

$$B_r = B_s\Big(\frac{R_s}{r}\Big)^2, \tag{1}$$

and

$$B_T(r,\theta) = B_s \sin\theta \frac{v_{\rm rot}}{v_{\rm sw}}\Big(\frac{R_s}{r}\Big)^2\Big(\frac{r}{R_s}-1\Big), \tag{2}$$

where $v_{\rm sw}$ is the super wind speed, assumed to be in the radial direction, θ the polar angle ($\theta = 0, \pi$), $B_{\rm s}$ the field at the stellar surface, R_s the stellar radius and $v_{\rm rot}$ the surface rotational velocity in the equatorial plane.

We define δ, the ratio of the magnetic energy $E_B = B^2/8\pi$ to the kinetic energy $E_k = \rho_{\rm sw}(v_{\rm sw})^2/2$,

$$\delta = 2.36\times10^{-3}\frac{(\frac{B}{10^{-2}G})^2\,(\frac{r}{1{\rm AU}})^2}{(\frac{\dot{M}}{10^{-7}M_\odot{\rm yr}^{-1}})\,(\frac{v_{\rm sw}}{10\,{\rm km\ s}^{-1}})}. \tag{3}$$

If $\delta > 10^{-4}$, then the magnetic field is dynamically important and has the potential to dominate the motion of the gas. For example for an observed magnetic field of $\sim 10^{-3}$ at $r \sim 1000$ AU we have $\delta \sim 0.236$. Then we assume that the magnetic field plays an auxiliary role for shaping PNe.

3 THEORETICAL MODELS

Considering that radius of a PN is so bigger than its thickness we can use the thin shell approximation for its dynamic. The basic derivation of the dynamic equations in the generalized thin- shell approximation is the conservation of mass and momentum within a control volume (CV). Giuliani (1982) has given a detailed treatment of the thin shell approximation for axisymmetric flow that we use here in the limit of an infinitesimally thin shell. In spherical polar coordinates the equations are

$$\tan\eta = -\frac{1}{R}\frac{\partial R}{\partial\theta}, \tag{4}$$

$$u_\parallel = -\frac{\partial R}{\partial t}\sin\eta, \qquad u_\perp = -\frac{\partial R}{\partial t}\cos\eta, \tag{5}$$

$$\frac{\partial\mu}{\partial t} = \rho(u_\perp - v_{a\perp}) - \frac{2\mu}{R}\frac{\partial R}{\partial t} - \mu\tan\eta\frac{\partial\eta}{\partial t} - \frac{\cos\eta}{R^2\sin\theta}\frac{\partial}{\partial\theta}[R\sin\theta\mu(v_\parallel - u_\parallel)], \tag{6}$$

$$\mu\frac{\partial v}{\partial t} = \rho(u_\perp - v_{a\perp})(v - v_a) + \hat{e}_\perp(P_i + \frac{B_i^2}{8\pi} - (v_\parallel - u_\parallel)\mu\frac{\cos\eta}{R}\frac{\partial v}{\partial\theta}, \tag{7}$$

where R is the PN radius, η the angle between the radius vector and the normal to the shell surface, ρ the PN density, μ its surface density and v_a the velocity of surrounding material. The ambient density ρ is one of the important parameters at the shell position. We assume that this density depends on the polar angle, θ, i.e it increases from the pole to the equator. Thus, we use the following form of density (Khesali & Ghanbari 2001),

$$\rho = \frac{\dot{M}_{\rm sw}}{4\pi v_{{\rm sw}_\circ}R_\circ^2}(1+\epsilon\sin^n\theta)\Big(\frac{\rm R_\circ}{\rm R}\Big)^2, \tag{8}$$

where $v_{{\rm sw}_\circ}$ is the super wind velocity at $\theta = 0$, as mass loss rate, $\dot{M}_{\rm sw}$, is independent of time and space, and the integer n and the parameter ϵ are free parameters characterizing the density distribution function.

Also we suppose the following time dependence of the surface density:

$$\mu(\theta, t) = \mu_s(\theta)\Big(\frac{t_\circ}{t}\Big). \tag{9}$$

The shape of the shell is repeated similarly at successive times, as the PN boundary moves with a constant velocity in interstellar medium. We describe the inner pressure factor as

$$P_i + \frac{B_i^2}{8\pi} = P_w + P_B\,, \tag{10}$$

which creates the PN expansion. The bubble pressure at the early stage is

$$P_w = \frac{\dot{M}_{\rm sw}}{4\pi v_{\rm sw} t^2}. \tag{11}$$

Since stellar radii are typically $\leq 10^{12}$ cm so we have $\frac{B_T}{B_r} \geq 10^2$ and possibly much larger in the region of interest, we have $B \approx B_T$ (Chevalier 1994). Hence we have

$$B_T(r,\theta) \approx B_s \sin\theta \frac{v_{\rm rot}}{v_{\rm sw}}\Big(\frac{R_s}{r}\Big)\,. \tag{12}$$

If we suppose $r = \Delta v_{\rm sw}(\theta) t$ with Δ a free parameter, then we have

$$P_B = \Big(B_s \sin\theta \frac{v_{\rm rot}}{\Delta v_{\rm sw}^2(\theta)} R_s\Big)^2 \frac{1}{8\pi t^2}\,. \tag{13}$$

Now from Equations (4)–(7) and (8)–(12) we have

$$\tan\eta = -\frac{1}{v_{\rm sw}(\theta)}\frac{\partial v_{\rm sw}(\theta)}{\partial\theta}\,, \tag{14}$$

$$\mu_s(\theta) = \frac{\dot{M}_{\rm sw}}{4\pi v_{\rm sw}\Delta^2 t_\circ}(1+\epsilon\sin^n\theta)\frac{\Delta v_{\rm sw}(\theta) - v_a}{v_{\rm sw}^2(\theta)}\cos\eta - \frac{\cos\eta}{v_{sw}^2(\theta)\sin\theta}\times$$
$$\frac{\partial}{\partial\theta}[v_{\rm sw}(\theta)\sin\theta\mu_s(\theta)(v_\parallel + \Delta v_{\rm sw}(\theta))\sin\eta]\,, \tag{15}$$

$$0 = -\frac{\dot{M}_{\rm sw}}{4\pi v_{sw_\circ}}(1+\epsilon\sin^n\theta)\Big[1 - \frac{v_a}{\Delta v_{\rm sw}(\theta)}\Big]^2\cos^2\eta\frac{\dot{M}_{\rm sw}}{4\pi v_{sw_\circ}} + \frac{1}{8\pi}\Big(B_s\sin\theta\frac{v_{\rm rot}}{\Delta v_{\rm sw}^2(\theta)}R_s\Big)^2$$
$$-(v_\parallel + \Delta v_{\rm sw}(\theta)\frac{\sin\eta)\cos\eta t_\circ}{\Delta v_{\rm sw}(\theta)}\times\mu_s\Big[\frac{\partial}{\partial\theta}(\Delta v_{\rm sw}(\theta)\cos\eta) - v_\parallel\Big(1+\frac{\partial\eta}{\partial\theta}\Big)\Big]\,, \tag{16}$$

$$0 = -\frac{\dot{M}_{\rm sw}}{4\pi v_{sw_\circ}}(1+\epsilon\sin^n\theta)\Big[1 - \frac{v_a}{\Delta v_{\rm sw}(\theta)}\Big](v_\parallel + v_a\sin\eta) - (v_\parallel + \Delta v_{\rm sw}(\theta)\sin\eta)\times$$
$$\frac{\mu_s t_\circ}{\Delta}\Big[\frac{\partial v_\parallel}{\partial\theta} + \Delta v_{\rm sw}(\theta)\cos\eta(1+\frac{\partial\eta}{\partial\theta})\Big]. \tag{17}$$

Equations (14)–(17) are a set of equations in the variables $v_{\rm sw}(\theta)$, $\eta(\theta)$, $\mu_s(\theta)$ and $v_\parallel(\theta)$. We can make these equations dimensionless by defining

$$v_{\rm sw}(\theta) = v_{\rm sw_\circ} X\,, \tag{18}$$

$$\mu_s(\theta) = \frac{\dot{M}_{\rm sw}}{4\pi v_{\rm sw_\circ}^2 t_\circ \Delta^2}(1+\epsilon\sin^n\theta)Y\,, \tag{19}$$

$$v_\parallel(\theta) = v_{\rm sw_\circ} Z\,, \tag{20}$$

where X, Y, Z are dimensionless variables. If we let $\lambda = \frac{v_a}{v_{\mathrm{sw}\circ}}$ we have

$$\frac{\partial X}{\partial \theta} = -X \tan\eta \,, \tag{21}$$

$$\frac{\partial \eta}{\partial \theta} = \frac{\cos^2\eta(1-\frac{\lambda}{X\Delta})^2 - \frac{1}{X(1+\epsilon\sin^n\theta)}[1+\frac{\sin^2\theta}{2X^3\dot{M}_{\mathrm{sw}}}(\frac{B_s v_{\mathrm{rot}} R_s}{\Delta v_{sw\circ}^2})^2]}{(Z+X\Delta\sin\eta)^2 Y\frac{\cos\eta}{X\Delta^3}} - 1\,, \tag{22}$$

$$\frac{\partial Z}{\partial \theta} = \frac{-(1-\frac{\lambda}{\Delta X})(Z+\lambda\sin\eta)\Delta^3}{(Z+\Delta X\sin\eta)Y} - X\Delta\cos\eta(1+\frac{\partial\eta}{\partial\theta})\,, \tag{23}$$

$$\begin{aligned}\frac{\partial Y}{\partial \theta} = &-\frac{Y}{Z+\Delta X\sin\eta}\frac{\partial Z}{\partial\theta} - \frac{XY\Delta}{Z+X\Delta\sin\eta}\cos\eta\frac{\partial\eta}{\partial\theta} + \frac{XY(\Delta\sin^2\eta-1)}{(Z+X\Delta\sin\eta)\cos\eta}\\ &+\frac{X\Delta-\lambda}{(Z+X\Delta\sin\eta)X} + Y(\tan\eta-\cot\theta) - \frac{n\epsilon\sin^{n-1}\theta}{1+\epsilon\sin^n\theta}\,.\end{aligned} \tag{24}$$

By solving this set of equations, we can obtain quantities like curvature, tangent velocity, surface density, and shell radius.

4 APPLICATION FOR PNe

Planetary nebulae are plausible candidates for the present theory because they have a large ratio of stellar wind velocity to nebular velocity and frequently show axisymmetric shapes.

The central star wind velocity with a range of 600–4000 km s^{-1} is typically 2000 km s^{-1} (Grewing 1988) and the nebular velocity with a range of 10–40 km s^{-1} is typically 20 km s^{-1}. The stellar mass loss rate is $\dot{M}_{\mathrm{sw}} = 9.5\times10^{17}$ kg s^{-1}. The nuclei of PNe ultimately evolve to white dwarfs, of which 2%–3% are found to have strong magnetic fields in the range $10^7 - 10^8$ G (Schmidt 1989). However, the remainder may have relatively weak fields with $B_s < 10^5$ G. The nuclei of PNe are considerably more extended than white dwarfs and still have a small amount of envelope material. Asymmetric nebulae with spherical halos warrant further investigation in terms of the magnetic shaping model.

The presented calculations show that a wide range of axisymmetric shapes can be obtained by varying the magnetic field density, the ambient wind velocity, λ, and other parameters of the density such as $\dot{M}_{\mathrm{sw}}$ and v_{sw}. In order to account the above assumptions and set of Equations (21)–(24) we generally require numerical calculations of the following physical quantities; the shell radius at the pole and equator, the shell velocity, the shell density, and other physical quantities throughout the entire nebula. The numerical calculations were done using the code 'PNFB' written in Matlab environment.

First of all by assuming $A = \frac{B_s^2 v_{\mathrm{rot}}^2 R_s^2}{2\dot{M}_{\mathrm{sw}}\Delta^2 v_{\mathrm{sw}\circ}^4}$ in Equation (22) and $\epsilon = 1$, $n = 2$, $\lambda = 0.5, \Delta = 3$, we consider the effect of changing A on the PN structure while keeping all other parameters constant. See Figure 1. For $A = 0$ which means zero magnetic pressure, the radius steadily decreases from pole to equator. With increasing A, the radius increases at all angles but more at the equator, so the ratio of polar to equatorial radius decreases.

Figure 2 shows the variation of density with the polar angle for the same different values of A and constant parameters as in Figure 1. For a given A, the density increasing with increasing polar angle. At the equator the density decreases with increasing A. The figure also shows how the density changes as Δ changes.

Figure 3 shows the corresponding variations in the super wind velocity. We can see how the velocity is affected by the magnetic field via the density distribution function and by the value of Δ. Recall that η is the angle between the radial vector and the normal of the shell surface, so it is a measure of the asphericity of the shell. Figure 4 shows that, at a given θ, η decreases with increasing A.

Figure 5 shows the shell profile for fixed values of λ, A, Δ and different values of n, ϵ. Clearly, an increase in n at constant ϵ leads to increase in expansion velocity relative to the equator, hence an increase in the shell asphericity. Also, at constant n, an increased ϵ with movement to the equator, the expansion velocity decreases and therefore the shell shape will be altered accordingly.

At last by comparing our results to those of Khesali & Ghanbari (2003), we can say that a magnetic field in a PN can affect its shape and symmetry.

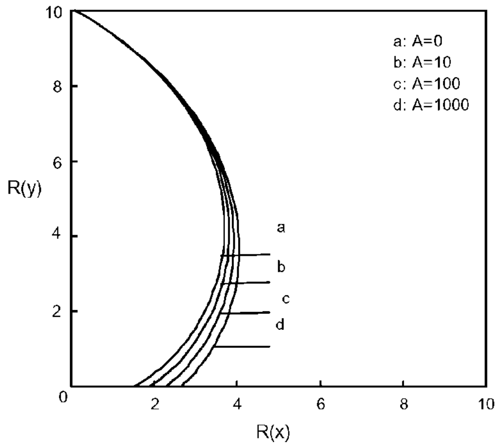

Fig. 1 Shape of shell for different values of A, the other parameters are fixed at $\epsilon = 1$, $n = 2$ and $\lambda = 0.5$.

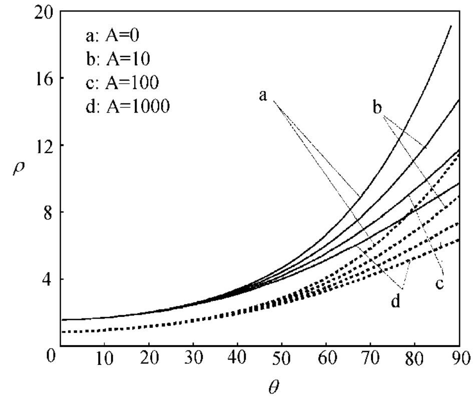

Fig. 2 Variation of density with polar angle for different values of A and the other parameters are chosen to be $\epsilon = 1$, $n = 2$, $\lambda = 0.5$. Full lines for $\Delta = 7$ and dotted lines for $\Delta = 3$.

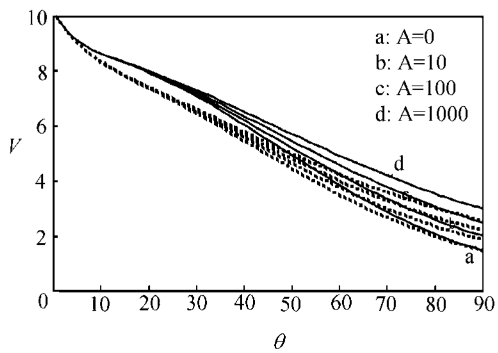

Fig. 3 Variation of super wind velocity with the polar angle for different values of A. Full lines for $\Delta = 7$ and dotted lines for $\Delta = 3$.

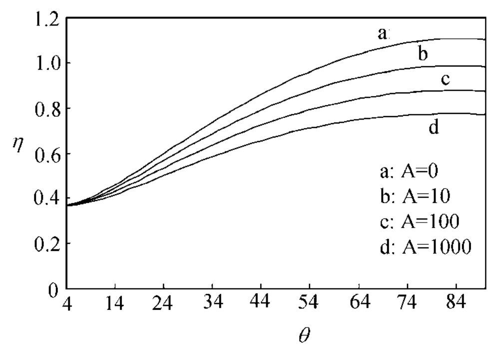

Fig. 4 Variation of asphericity of the shell (η) with the polar angle for same different values of A, and constant parameters as in Fig. 1.

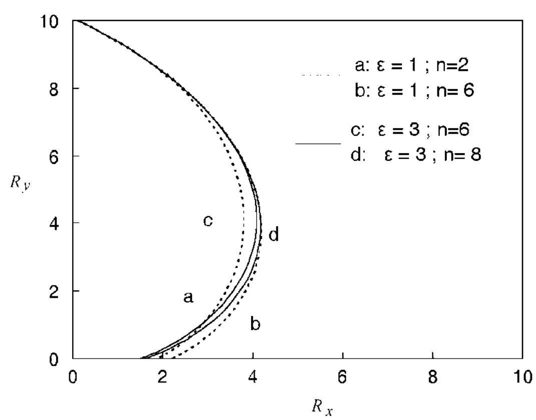

Fig. 5 Shape of shell for different values of λ, the other parameters are chosen to be $\Delta = 7$ and $A = 0.5$.

5 SUMMARY

The reason of why more than 80% of the known planetary nebulae are bipolar and not spherically symmetric is barely understood. Jordan et al. (2005) have shown in their works that magnetic fields exist in the central stars of planetary nebulae. This discovery supports the idea that magnetic fields are important for the non-spherical shape of most planetary nebulae. We consider the interacting stellar winds model (Kwok et al. 1978), where the fast wind $(v_{\rm fw} \approx 1000\,{\rm km\,s^{-1}}$, mass loss rate $10^{-7}\,M_{\odot}\,{\rm yr}^{-1}$ from the central star of a PN encounters an older slow wind $(v_{\rm sw} \approx 10{\rm km\,s^{-1}})$ from an earlier phase with heavy mass loss $(10^{-5}M_{\odot}$ yr). We assume that the magnetic field in the wind from a magnetized rotating star becomes increasingly toroidal with distance from the star. A fast wind shocks against the external medium and creates a bubble whose volume is dominated by the shocked gas. The toroidal magnetic field increases in the shocked bubble, leading to increase in magnetic pressure, and also a thermal pressure causes an increase in the expansion velocity. By numerical solutions of the dynamical equations we calculated quantities like shell radius, shell density, and expansion velocity as functions of the polar angle for different values of the magnetic field. We can say that in addition to processes such as ionization and recombination that cause cooling and heating in the shell and play an important role in dynamical structure of PNe, the magnetic pressure is important as well. Therefore, in order to simulate PNe and compare its results with observational data, all of the factors such as heating and cooling and magnetic field should be considered.

Acknowledgements This work has been supported partially by the Research Institute of Astronomy and Astrophysics of Maragha, Iran.

References

Balick B., 1987, AJ, 94, 671
Blackman E. G., Frank A., Markiel J. A. et al., 2001, Nature, 409, 485
Chevalier R. A., Luo D., 1994 , ApJ, 421, 225
Etoka S., Diamond P., 2004, MNRAS, 348, 34
García-Segura G., Langer N., Rozycka M., Franco J., 1999, ApJ, 517, 767
Ghanbari J., and Khesali A. R., 2001, Ap&SS, 278, 391
Giuliani J. L., Jr. 1982, ApJ, 256, 624
Grewing M., 1988, In: S. Torrespeimbert, ed., IAU Symp. 131, Planetary Nebulae, Dordrecht: Kluwer, p.241
Jordan S., Werner K., O'Toole S. J., 2005, A&A, 432, 273
Khesali A. R., Ghanbari J., 2003, Ap&SS, 288, 465
Kwok S., Purton C. R., Fitzgerald P. M., 1978, ApJ, 219, L125
Matt S., Balick B., Winglee R., Goodson A., 2000, ApJ, 545, 965
Pascoli G., 1997, ApJ, 489, 946
Perinotto M., 1983, IAUS, 103, 323P
Schmidt G., 1989, In: IAU Coll. 114, White Dwafs, ed. G. Wegner, Dordrecht: Kluwer, p.305
Soker N., 2006, The Publications of the Astronomical Society of the Pacific, Vol. 118, Issue 840, pp.260–269